ELSEVIER

Journal of Molecular Catalysis A: Chemical 169 (2001) 67–78

JOURNAL OF MOLECULAR CATALYSIS A: CHEMICAL

www.elsevier.com/locate/molcata

Hydroformylation of 1-hexene and propene with in situ formed rhodium phosphine catalysts

Pekka Suomalainen [a], Heidi K. Reinius [b], Helena Riihimäki [c], Riitta H. Laitinen [c], Sirpa Jääskeläinen [a], Matti Haukka [a], Jouni T. Pursiainen [c], Tapani A. Pakkanen [a,*], A.O.I. Krause [b]

[a] *Department of Chemistry, University of Joensuu, P.O. Box 111, FIN-80101 Joensuu, Finland*
[b] *Department of Chemical Technology, Helsinki University of Technology, P.O. Box 6100, FIN-02015 HUT, Finland*
[c] *Department of Chemistry, University of Oulu, P.O. Box 3000, FIN-90401 Oulu, Finland*

Received 4 September 2000; received in revised form 7 December 2000; accepted 7 December 2000

Abstract

A series of triphenylphosphines modified with different heteroatom groups (–SCH_3, –$N(CH_3)_2$, –OCH_3, –CF_3) in *ortho* or *para* position of the phenyl ring(s) were synthesised and tested for their catalytic behaviour in the rhodium catalysed hydroformylation of 1-hexene (80°C, 15 bar) and propene (100°C, 10 bar). Hydroformylation results for 1-hexene and propene differed markedly. With 1-hexene, the differences in activity and in chemo- and regioselectivity obtained with the various ligands were minor. Among the heterodonor ligands, the strong σ-donor ligands yielded higher hydroformylation activity than the less basic ligands. In the case of propene, heterodonor bidentate ligands suppressed the hydroformylation reaction. In addition, 1,4-bis(diphenylphosphino)butane and (*o*-thiomethylphenyl)bis(1-naphthyl)phosphine favoured the formation of *n*-butanal. Only the –CF_3 modified ligands behaved similarly with the two alkenes. The influence of the structure of the ligand in hydroformylation was studied by using molecular modelling methods. The steric size of the ab initio energy minimised free ligand structures was evaluated by Tolman's cone angle method. Co-ordination properties of –CF_3 group modified phosphines were studied in reaction with $Rh_2(CO)_4Cl_2$, and the structure of $Rh(CO)Cl(P(o\text{-}CF_3C_6H_4)Ph_2)_2$ (**1**) was determined crystallographically.

Keywords: Hydroformylation; Rhodium; Phosphine ligands; Propene; 1-Hexene

1. Introduction

Geometrical arrangement of ligands around the metal centre plays an important role in homogeneous organometallic catalysis. The selectivity of catalytic reactions can be modified through tailoring of the catalyst sphere by sophisticated ligand design. Although the influence of different phosphorus ligands on hydroformylation reaction has been studied for decades, a satisfactory explanation for the consistent correlation between catalytic activity and the geometry of the ligands has yet to be provided [1]. Aldehydic regioselectivity is more predictable, and clear trends are obtained at least within a small set of structurally similar ligands. Perhaps as the best example, the size of the natural biting angle of the diphosphine ligand, i.e. the P–M–P angle, can be used as a tool to steer the product distribution of the hydroformylation

* Corresponding author. Tel.: +358-13-2513345; fax: +358-13-2513344.
E-mail address: tapani.pakkanen@joensuu.fi (T.A. Pakkanen).

1381-1169/01/$ – see front matter
PII: S1381-1169(01)00038-3

reaction [2,3]. Regioselective control to branched product has been reported in the hydroformylation of 3,3,3-trifluoropropene [4] and some functional alkenes [5,6], but in these approaches, tailoring was assisted by substituting one end of the alkene with a fluoro, phosphine or silyl group.

We have recently shown [7] that in the hydroformylation of methyl methacrylate (MMA) regioselective control to branched product can be obtained through chelation control with an in situ formed (*o*-thiomethylphenyl)diphenylphosphine rhodium complex. We also showed [8] that the complex formation of various heterodonor phosphine ligands with rhodium differed depending on the σ-donor group. It has further been argued that the alkene itself — especially if polar like MMA or if able to isomerise simultaneously — might affect the regioselective control. In the case of 1-hexene hydroformylation (Fig. 1), isomerisation is dominant, yielding less reactive 2- and 3-hexenes [9]. Regardless of the preference for either normal product (1-heptanal) or the branched products (2-methylhexanal or 2-ethylpentanal), the isomerising capability of the catalyst needs to be clarified. If the normal product is desired the catalyst should not exhibit isomerising tendency, whereas if branched products are desired the catalyst should first isomerise the alkene and thereafter be able to effectively hydroformylate the isomers. Regioselectivity is also strongly dependent on the nature of the substrate. Trzeciak and Ziolkowski [10] showed that the general tendencies observed for the hydroformylation of 1-hexene with a phosphite modified rhodium catalyst also apply to propene, but that there were essential differences in the *n*:*i* ratios.

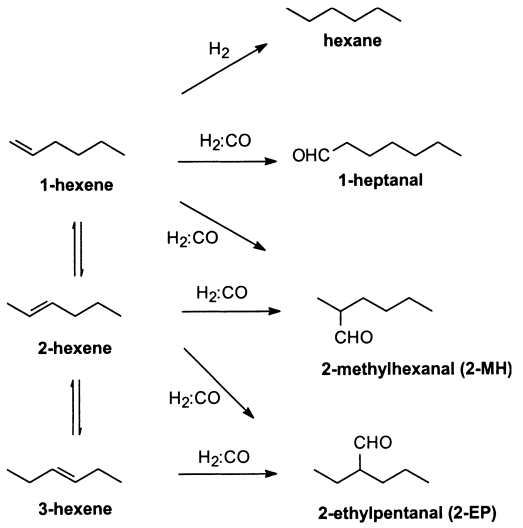

Fig. 1. Hydroformylation of 1-hexene.

Here we report the effects of phosphine ligands differing in stereoelectronic properties on the hydroformylation of propene and 1-hexene. Although, different precursors and reaction conditions were applied for the two alkenes their mutual comparison is reasonable as the effects of different ligands were examined relative to PPh_3 modified reaction. Furthermore, the use of different Rh-species were sought to be justified, as the formation of actual catalyst species, trigonal bipyramidal rhodium carbonyl hydride, can be formed from various rhodium precursors.

The phosphine ligands were triphenylphosphine-type ligands modified in *ortho* or *para* position with different heterodonor groups ($–SCH_3$, $–N(CH_3)_2$, $–OCH_3$ or $–CF_3$). In addition, the phenyl ring was replaced with a naphthyl or anthracene group to increase the steric stress. Geometries of the free ligands were calculated by ab initio Hartree–Fock method and the sizes of the geometry optimised free ligand structures were measured with Tolman's cone angle method [11]. Complexation studies with rhodium and the ligands containing ($–CF_3$) groups were also carried out.

2. Experimental

2.1. Ligands

2.1.1. General comments

The commercial ligands used in the experiments were triphenylphosphine (PPh_3, Fluka, ∼99%) and 1,2-bis(diphenylphosphino)ethane (DPPE, Fluka, 98%) and 1,4-bis(diphenylphosphino)butane (DPPB, Fluka, >97%). The other ligands were prepared by literature methods (Table 1), except for the CF_3-substituted ligands (*o*-trifluoromethylphenyl) diphenylphosphine (*o*CF_3P), (*p*-trifluoromethylphenyl) diphenylphosphine (*p*CF_3P), tris(*o*-trifluoromethylphenyl)phosphine (*o*$(CF_3)_3$P) and tris(*p*-trifluoromethylphenyl)phosphine (*p*$(CF_3)_3$P), which were prepared by modified literature methods [12,13]. Commercially available reagents were used without

Table 1
Ligands used in the hydroformylation experiments

Abbreviation		Name	Reference
*o*SP	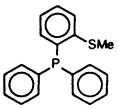	(*o*-Thiomethylphenyl)diphenylphosphine	[30]
*p*SP	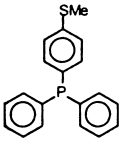	(*p*-Thiomethylphenyl)diphenylphosphine	[30]
*o*NP	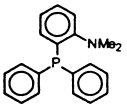	(*o*-*N*,*N*-dimethylaminophenyl)diphenylphosphine	[31]
*o*SeP	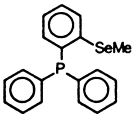	(*o*-Methylselenophenyl)diphenylphosphine	[32]
*o*OP	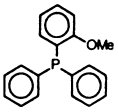	(*o*-Methoxyphenyl)diphenylphosphine	[30]
*o*SP(naf)$_2$	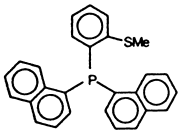	(*o*-Thiomethylphenyl)bis(1-naphthyl)phosphine	[33]
*o*OP(naf)$_2$	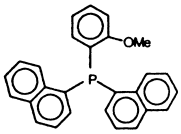	(*o*-Methoxyphenyl)bis(1-naphthyl)phosphine	[33]
*o*CF$_3$P		(*o*-Trifluoromethylphenyl)diphenylphosphine	[12]
*p*CF$_3$P	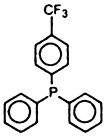	(*p*-Trifluoromethylphenyl)diphenylphosphine	[12]
o(CF$_3$)$_3$P	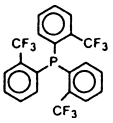	Tris(*o*-trifluoromethylphenyl)phosphine	[12]

Table 1 *(Continued)*

Abbreviation		Name	Reference
$p(CF_3)_3P$	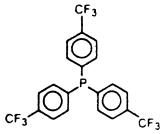	Tris(*p*-trifluoromethylphenyl)phosphine	[12]
$PPh(anthr)_2$	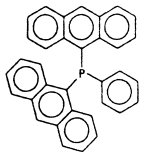	Bis(9-anthracenyl)phenylphosphine	[34]
$PPh_2(anthr)$	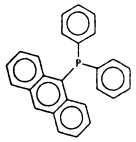	(9-Anthracenyl)diphenylphosphine	[34]

further purification. Diethyl ether (Lab Scan) was distilled from sodium/benzophenone ketyl under nitrogen before use. All ligand syntheses were carried out with standard Schlenk techniques under nitrogen or an argon atmosphere.

2.1.2. Spectroscopy

Characterisation of the ligands was based mainly on ^{1}H, ^{13}C–$\{^{1}H\}$ and ^{31}P–$\{^{1}H\}$ NMR spectroscopy. NMR spectra were recorded on Bruker AM200 and DPX400 spectrometers at room temperature in $CDCl_3$. ^{1}H NMR: reference $SiMe_4$. ^{13}C–$\{^{1}H\}$ NMR: $CDCl_3$ set to 77.0 ppm. ^{31}P–$\{^{1}H\}$ NMR: external standard 85% H_3PO_4. Two-dimensional HSQC NMR spectra were also measured. Exact mass peaks were determined on a Micromass LCT, ESI+.

2.1.3. Synthetic procedure for CF_3-modified ligands

To 2-bromobenzotrifluoride (Aldrich, 99%) or 4-bromobenzotrifluoride (Aldrich, 99%) in 30 ml diethyl ether was added *n*-butyllithium (Aldrich, 2.5 M solution in hexane) in 20 ml diethyl ether at −10 to 0°C (ice bath). The mixture was stirred for 1.5 h at −10 to 0°C, after which a solution of diphenylchlorophosphane (Aldrich, 95%) or phosphorus trichloride (Merck, 99%) in 30 ml of diethyl ether was added drop-wise. The mixture was stirred at −10 to 0°C for 1.5 h. After slowly warming to room temperature, the layers were separated and the solvent was removed in vacuo.

2.1.4. (o-Trifluoromethylphenyl)diphenylphosphine (oCF_3P)

When a solution of *n*-butyllithium (10 ml, 25 mmol) in diethyl ether was added to a solution of 2-bromobenzotrifluoride (5.63 g, 25 mmol) in diethyl ether, the reaction mixture turned to red. Addition of a solution of diphenylchlorophosphine (5.52 g, 25 mmol) in diethyl ether coloured the reaction mixture brown. The yield of the brown solid product was 96.9% (8.00 g, 24.2 mmol). ^{1}H NMR (200 MHz, $CDCl_3$): δ 7.19–7.29 (m, 7H, H^6, H^8 and H^{10}), 7.30–7.37 (m, 4H, H^9), 7.41–7.47 (m, 2H, H^4 and H^5), 7.72–7.80 (m, 1H, H^3). ^{13}C–$\{^{1}H\}$ NMR (100 MHz, $CDCl_3$): 124.34 (q, $^{1}J_{C-F}$ = 275.7 Hz, 1C, C^{11}), 126.40 (s, 1C, C^3), 128.56 (d, $^{3}J_{C-P}$ = 6.3 Hz, 4C, C^9), 128.83 (s, 2C, C^{10}), 128.94 (s, 1C, C^5), 131.58 (s, 1C, C^4), 133.68 (d, $^{2}J_{C-P}$ = 19.1 Hz, 4C, C^8), 134.94 (d, $^{1}J_{C-P}$ = 29.9 Hz, 1C, C^1), 136.08 (s, 1C, C^6), 134.00–137.00 (m, 2C, C^1 and C^2), 136.44 (d, $^{1}J_{C-P}$ = 11.3 Hz, 2C, C^7). ^{31}P–$\{^{1}H\}$ NMR (161 MHz, $CDCl_3$): −9.35 (q, $^{4}J_{P-F}$ = 53.3 Hz, 1P). TOF MS ES+ calc. for $(M + Na)^+$ ($C_{19}H_{14}F_3NaP$) 353.0683, found 353.0717.

2.1.5. Tris(o-trifluoromethylphenyl)phosphine ($o(CF_3)_3P$)

When a solution of *n*-butyllithium (10 ml, 25 mmol) in diethyl ether was added to a solution of 2-bromobenzotrifluoride (5.63 g, 25 mmol) in diethyl ether, the reaction mixture turned orange. Addition of a solution of phosphorus trichloride (1.14 g, 8.3 mmol) in diethyl ether coloured the reaction mixture to brown. The yield of the brown solid product was 92.3% (3.59 g, 7.69 mmol). ^{1}H NMR (400 MHz, $CDCl_3$): δ 6.93 (dd, $^3J_{H-H} = 7.4$ Hz, $^3J_{H-P} = 3.4$ Hz, 3H, H^6), 7.43 (t, $^3J_{H-H} = 7.4$ Hz, 3H, H^4), 7.49 (t, $^3J_{H-H} = 7.4$ Hz, 3H, H^5), 7.75–7.80 (m, 3H, H^3). ^{13}C–{^{1}H} NMR (100 MHz, $CDCl_3$): 124.06 (q, $^1J_{C-F} = 275.3$ Hz, 3C, C^{11}), 127.03 (s, 3C, C^3), 129.32 (s, 3C, C^5), 131.63 (s, 3C, C^4), 134.27 (q, $^2J_{C-F} = 29.8$ Hz, 3C, C^2), 134.84 (d, $^1J_{C-P} = 29.8$ Hz, 3C, C^1), 136.02 (s, 3C, C^6). ^{31}P–{^{1}H} NMR (161 MHz, $CDCl_3$): −15.60 (q, $^4J_{P-F} = 55.3$ Hz, 1P). TOF MS ES+ calc. for $(M + Na)^+$ ($C_{21}H_{12}F_9NaP$) 489.0431, found 489.0445.

2.1.6. Tris(p-trifluoromethylphenyl)phosphine ($p(CF_3)_3P$)

When a solution of *n*-butyllithium (9.4 ml, 23.3 mmol) in diethyl ether was added to a solution of 4-bromobenzotrifluoride (5.25 g, 23.3 mmol) in diethyl ether, the reaction mixture turned red. Addition of a solution of phosphorus trichloride (1.07 g, 7.8 mmol) in diethyl ether caused the reaction mixture to turn orange. When the orange oily product was washed with hexane and cooled (−20°C) an orange solid product precipitated. The yield of the product was 67.6% (2.45 g, 5.25 mmol). ^{1}H NMR (400 MHz, $CDCl_3$): δ 7.41 (t, $^3J_{H-H} = 7.8$ Hz, 6H, H^2), 7.63 (d, $^3J_{H-H} = 8.0$ Hz, 6H, H^3). ^{13}C–{^{1}H} NMR (100 MHz, $CDCl_3$): 123.82 (q, $^1J_{C-F} = 272.4$ Hz, 3C, C^9), 125.64 (s, 6C, C^3), 131.55 (q, $^2J_{C-F} = 32.7$ Hz, 3C, C^4), 134.96 (d, $^3J_{C-P} = 30.8$ Hz, 6C, C^2), 140.26 (d, $^1J_{C-P} = 14.1$ Hz, 3C, C^1). ^{31}P–{^{1}H} NMR (161 MHz, $CDCl_3$): −4.29 (s). TOF MS ES+ calc. for $(M + H)^+$ ($C_{21}H_{13}F_9P$) 467.0611, found 467.0639.

2.1.7. Computational details

Gaussian 94 [14] and Sybyl [15] programs were used in modelling. Geometric optimisations at the Hartree–Fock level were done using the 3-21G* basis set. The steric size of the prepared phosphine ligands was estimated by Tolman's cone angle method. Metal(dummy atom)-phosphorus distance 2.28 Å and the van der Waals radii of hydrogen 1.2 Å were used in cone angle determinations.

2.2. Complex synthesis

Synthetic reactions were carried out using standard Schlenk techniques in nitrogen atmosphere. The solvents, methanol and toluene (p.a. grade), were deoxygenated with nitrogen before use. $Rh_2(CO)_4Cl_2$ was prepared according to a literature method [16]. NMR spectra were recorded on a Bruker AM250 spectrometer. ^{31}P NMR spectra were referenced to 85% H_3PO_4. Elemental analyses were recorded on a Perkin-Elmer 2400 Series II CHNS/O analyser.

*2.2.1. Preparation of $Rh(CO)Cl(oCF_3P)_2$ (**1**)*

$Rh_2(CO)_4Cl_2$ (25 mg, 0.064 mol) and oCF_3P (42 mg, 0.127 mol) were dissolved in methanol in separate flasks. The ligand solution was added drop-wise to the solution of the rhodium compound. The yellow precipitate was filtered, washed with methanol and dried quickly under vacuum. Yellow crystals for X-ray studies were grown from CH_2Cl_2. Elemental analysis for **1** $C_{39}H_{28}P_2F_6OClRh$: calc. % C, 56.65; H, 3.41; found % C, 56.40; H, 3.40. IR: υ(CO) = 1977 cm^{-1}. ^{31}P NMR: $\delta = 37.5$ ppm, J(Rh–P) = 136 Hz.

*2.2.2. Preparation of $[Rh(CO)Cl(p(CF_3)_3P)]_2$ (**2**)*

A similar procedure as for **1** was used for **2**. Starting form $Rh_2(CO)_4Cl_2$ (25 mg, 0.064 mol) and $p(CF_3)_3P$ (60 mg, 0.129 mol). Elemental analysis for **2** $C_{44}H_{24}P_2F_{18}O_2Cl_2Rh_2$: calc. % C, 41.77; H, 1.91; found % C, 41.70; H, 1.79. IR: υ(CO) = 1999 cm^{-1}. ^{31}P NMR: $\delta = 46.9$ ppm, J(Rh–P) = 170 Hz.

2.3. X-ray crystallography

X-ray diffraction data were collected with a Nonius KappaCCD diffractometer using Mo Kα radiation ($\lambda = 0.71073$ Å). Denzo and Scalepack [17] programs were used for cell refinements and data reduction. The structure was solved by direct methods using the SIR97 [18] program with the WinGX [19] graphical user interface. The structure refinement was carried out with SHELXL97 [20]. A multi-scan absorption correction, based on equivalent reflections (XPERP in

Table 2
Crystallographic data for **1**

Empirical formula	$C_{39}H_{28}ClF_6OP_2Rh$
Molecular weight	826.91
Crystal size (mm)	0.30 × 0.20 × 0.10
Crystal system	Monoclinic
Space group	$P2_1/n$
λ (Å)	0.71073
a (Å)	11.4595(4)
b (Å)	11.1631(5)
c (Å)	13.8105(5)
β (°)	100.965(2)
V (Å^3)	1734.43(12)
Z	2
D_{calc} (g/cm^3)	1.583
μ (mm^{-1})	0.726
T (°C)	120
θ range (°)	2.36–26.03
No. of unique reflections	3278
No. of observed data[a]	2672
No. of parameters	226
R_1	0.0327
wR^2	0.0662
Largest different peak and hole (e/Å^3)	0.698 and −0.451

[a] $I > 2\sigma$.

Table 3
Interatomic bond distances and angles for **1**

Atoms	Bond distances (Å)
Rh(1)–C(21)	1.722(8)
Rh(1)–P(1)	2.332(6)
Rh(1)–Cl(1)	2.408(3)
O(21)–C(21)	1.148(9)
P(1)–C(13)	1.821(3)
P(1)–C(7)	1.826(3)
P(1)–C(1)	1.851(3)
C(2)–C(19)	1.505(4)
F(1)–C(19)	1.334(3)
C(21)–Rh(1)–P(1)	87.6(2)
P(1)–Rh(1)–Cl(1)	86.97(5)
Cl(1)–C(21)–Rh(1)	176.2(8)
O(21)–C(21)–Rh(1)	176.3(6)
C(13)–P(1)–Rh(1)	109.10(9)
C(7)–P(1)–Rh(1)	123.23(9)
C(1)–P(1)–Rh(1)	112.82(8)
C(21)–Cl(1)–Rh(1)	2.7(6)
C(13)–P(1)–C(7)	102.21(1)
C(13)–P(1)–C(1)	103.76(1)
C(7)–P(1)–C(1)	103.67(1)
F(1)–C(19)–C(2)	112.5(2)
F(1)–C(19)–F(3)	106.3(2)

SHELXTL, version 5.1) [21], was applied to the data (T_{min}/T_{max} = 0.2271/0.2764). CO and Cl ligands were disordered in two-positions with equal population parameter 0.5. This type of disorder is typical for *trans*-triphenylphosphines (PPh)–Rh(CO)Cl–(PPh). Because of disorder, C(21), O(21) and Cl(1) were refined only isotropically. All hydrogens were constrained to ride on their parent atom. Crystallographic data are summarised in Table 2 and selected bond lengths and angles are given in Table 3. Crystallographic data (excluding structure factors) for the structure reported in this paper have been deposited with the Cambridge Crystallographic Data Centre as supplementary publication no. CCDC 145349. Copies of the data can be obtained free of charge on application to CCDC, 12 Union Road, Cambridge CB2 1EZ, UK. [1]

2.4. Hydroformylation of propene

Propene hydroformylation experiments were carried out in a 250 ml autoclave (Berghof) equipped with a sampling system and a 230 ml Teflon liner. The experiments were done in semi-batch mode. The rhodium precursor was $Rh(NO_3)_3{\cdot}2H_2O$ (Fluka). In a typical experiment, the autoclave was charged with the rhodium precursor (0.02 mmol calculated as rhodium), acetone (310 mmol, Merck, 99.5%), internal standards decane (7 mmol, Fluka, >98%) and hexane (12 mmol, Riedel de Häen, >99%), and the phosphine. If not otherwise stated, the ligand to rhodium ratio was 10:1 on molar basis. The system was first flushed with nitrogen, pressurised with propene (2 bar, Aga, >99.8%), heated to the reaction temperature (100°C) with continuous stirring, and then pressurised to the reaction pressure (10 bar) with a 1:1 molar ratio of H_2 and CO (MG, 99.997%). At least nine samples were taken for analysis in each experiment: one of the fresh reaction mixture, one immediately after pressurising with H_2 and CO, which was considered as the starting point of the reaction, six during the experiment and one after the reaction.

2.5. Hydroformylation of 1-hexene

1-Hexene hydroformylation reactions were conducted in a 100 ml autoclave (Berghof) with 60 ml

[1] Fax: +44-1223-336-033; e-mail address: deposit@ccdc.camac.uk.

Teflon liner. The experiments were carried out in batch mode with rhodium precursor $Rh_4(CO)_{12}$. The reactor was charged under a nitrogen purge with substrate, rhodium precursor, ligand, internal standard, cyclohexane and solvent (toluene). The autoclave was then sealed and pressurised using a 1:1 mixture of H_2 and CO (MG, 99.997%) to 15 bar and heated to 80°C. After 6 h the autoclave was cooled and brought to atmospheric pressure.

The reproducibility of the system was confirmed by accomplishing the tests twice. A disposable inner Teflon liner was used to avoid the accumulation of rhodium on the reactor walls. Furthermore, the purity of the system was checked with blank runs before each experiment. The products were analysed with a Hewlett-Packard 5890 GC equipped with a capillary column (HP-1, 1.0 μm × 0.32 mm × 60 m) and a flame-ionisation detector. Products were quantified by the internal standard method. In addition, the aldehydes that formed were identified by GC–MS analysis.

In the case of 1-hexene hydroformylation, the various catalysts were compared at equal conversion levels. With propene, conversion dependence was more straightforward: the isomerisation reforms the substrate and no hydrogenation products were detected. As Fig. 2 shows, in the hydroformylation of propene, the selectivity of the reaction did not depend on the conversion level and thus the comparison of the catalysts is valid even at different conversion levels.

3. Results

3.1. Properties of the ligands

The calculated and measured properties of the ligands are shown in Tables 4 and 5. The cone angles for the ligands varied from 149 to 221°. Cone angles of all the *ortho*-substituted ligands were larger than that of PPh_3 (149°), whereas cone angles of the analogous *para*-substituted ligands were similar in size to that of PPh_3 evidently because *para*-substituents did not directly affect the angle. However, since ligands exhibit a large flexibility range, cone angle calculations based on optimised free ligand structures may be insufficient for the estimation of steric requirements of the co-ordinated ligands. The values should nevertheless give a qualitative idea of the steric size of the ligand.

The electronegative effect of the substituents on phosphorus and the angles between the substituents are the two most important variables determining the ^{31}P NMR-shifts, and hence the shift reflects the stereoelectronic state of the phosphorus atom [11]. As Tables 4 and 5 show, the ^{31}P NMR-shift of the ligands varied markedly, from −3.3 to −31.9 ppm. Small, π-acceptor ligands were observed at high field while fairly large ligands with aromatic rings occupied lower field.

3.2. Hydroformylation tests

Tables 4 and 5 show the effect of different ligands on the 1-hexene and propene hydroformylation.

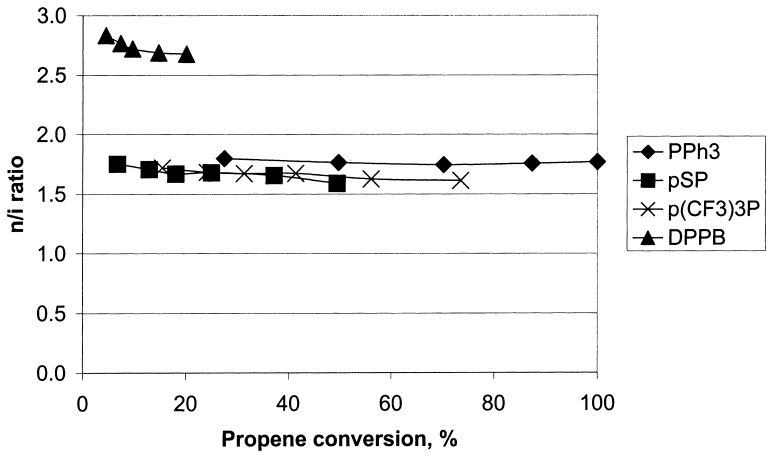

Fig. 2. Regioselectivity of propene hydroformylation as a function of propene conversion.

Table 4
Measured and calculated properties of the ligands and 1-hexene hydroformylation results[a]

Ligand	θ	^{31}P NMR-shift	Conversion (%)	$S_{2\text{-hexenes}}$ (%)	$S_{3\text{-hexenes}}$ (%)	$S_{2\text{-EP}}$ (%)	$S_{2\text{-MH}}$ (%)	$S_{1\text{-heptanal}}$ (%)	$S_{\text{total aldehydes}}$ (%)	*n*:*i* ratio
*o*SP	158	−12.9	88	62	19	1	7	11	19	1.4
*o*NP	180	−12.5	84	65	20	1	5	9	15	1.5
*o*OP	166	−15.6	86	67	19	1	5	9	14	1.7
*o*SP(naf)$_2$	166	−29.7	87	63	20	1	6	10	17	1.4
*o*OP(naf)$_2$	204	−31.9	84	68	19	0	5	9	14	2.0
oCF_3P	174	−9.4	0	0	0	0	0	0	0	0.0
pCF_3P	149	−4.1	0	0	0	0	0	0	0	0.0
p$(CF_3)_3$P	149	−4.3	88	58	18	2	9	12	23	1.1
PPh(anthr)$_2$	207	−27.7	87	62	20	1	7	10	18	1.2
PPh_2(anthr)	176	−22.9	79	64	20	1	6	9	16	1.3
PPh_3	149	−3.3	88	61	20	2	7	10	19	1.2
No ligand	–	–	86	60	19	2	8	11	20	1.1

[a] Condition: 80°C, 15 bar, 1-hexene:Rh = 10,000, L:Rh = 10, 6 h.

In general, in 1-hexene hydroformylation, fairly high isomerisation activity was associated with all ligands, and no hydrogenation was detected. Furthermore, the product distribution differed little from that of the unmodified and PPh_3 modified reactions. In every case, the major isomerisation product was 2-hexene. Moreover, with most of the ligands, the molar ratio of 2- to 3-hexenes was 3.1–3.2, which is close to that of the thermodynamic equilibrium (3.1) at 80°C [22,23]. Only for *o*OP and *o*OP(naf)$_2$ was the distribution of isomers further from the equilibrium: 3.5 and 3.6, respectively. In propene hydroformylation, the activity was highly dependent on the modifying ligand and the *n*:*i* ratio was always higher than that of the unmodified reaction.

3.2.1. σ-Donor ligands

The heterodonor ligand had a notable effect on the propene hydroformylation (Table 5). In some cases, small changes in the ligand structure resulted in total suppression of the reaction. Among the heterodonor ligands, only *o*NP, *p*SP and *o*SP(naf)$_2$ showed catalytic

Table 5
Measured and calculated properties of the ligands and propene hydroformylation results[a]

Ligand	θ	^{31}P-shift	L:Rh ratio	Conversion (%)	$S_{\text{isobutanal}}$ (%)	S_{butanal} (%)	*n*:*i* ratio
*o*SP	158	−12.9	10	0	0	0	0.0
			2	1	0	0	0.0
*p*SP	152	−4.7	10	49	39	61	1.7
*o*OP	166	−15.6	10	0	0	0	0.0
*o*SeP	–	−10.4	10	0	0	0	0.0
*o*NP	180	−12.5	10	98	40	60	1.5
DPPE	n.a.	–	10	0	0	0	0.0
DPPB	n.a.	–	10	20	27	73	2.7
oCF_3P	174	−9.4	10	0	0	0	0.0
			4	2	0	0	0.0
pCF_3P	149	−4.1	10	0	0	0	0.0
o$(CF_3)_3$P	221	−15.6	10	0	0	0	0.0
p$(CF_3)_3$P	149	−4.3	10	74	38	62	1.6
*o*SP(naf)$_2$	166	−29.7	10	15	29	71	2.4
PPh(anthr)$_2$	207	−27.7	10	9	36	64	1.8
PPh_3	149	−3.3	10	100	36	64	1.8
No ligand	–	–	–	5	50	50	1.0

[a] Condition: 100°C, 10 bar, propene:Rh = 3200, 4 h.

activity, with conversions of 98, 49 and 15%, respectively. Relative to the regioselectivity of PPh_3 (n:i = 1.8) *o*NP and *p*SP slightly enhanced the formation of isobutanal (n:i = 1.5 and 1.7), whereas *o*SP(naf)$_2$ favoured the formation of *n*-butanal (n:i = 2.4). Of the diphosphine ligands, DPPB favoured the formation of *n*-butanal (n:i = 2.7), whereas the analogue DPPE gave no conversion.

3.2.2. π-Acceptor ligands

Number and position of the CF_3 groups markedly affected the activity of the reaction with 1-hexene and propene (Tables 4 and 5). The addition of *o*CF_3P or *p*CF_3P blocked the reactions entirely, whereas *p*$(CF_3)_3$P showed good hydroformylation activity with both substrates. With 1-hexene, *p*$(CF_3)_3$P gave the best selectivity to aldehydes (23.4%), and the regioselectivity to the branched products (n:i = 1.1) was slightly better than that of the unmodified reaction. In propene hydroformylation, *p*$(CF_3)_3$P gave a fairly rapid reaction with similar regioselectivity to that of PPh_3 (n:i = 1.6 and 1.8, respectively). The catalyst modified with *o*$(CF_3)_3$P ligand gave no reaction in propene hydroformylation.

3.2.3. Steric effects

Increasing the steric stress of the ligand by replacing some of the phenyl rings with anthracyl rings had varied effects. Relative to PPh_3, in 1-hexene hydroformylation conversion drop was lower for PPh_2(anthr) ligand and, surprisingly, at the same level for the more bulky PPh(anthr)$_2$. The regioselectivity obtained with both anthracyl modified ligands resembled that of the PPh_3 modified reaction. Again relative to PPh_3, in propene hydroformylation. The replacement of two phenyl rings with anthracyl rings did not affect the regioselectivity but decreased the conversion.

3.3. Rh–P complexes

In view of unexpected behaviour of the –CF_3 ligand modified reactions, we proceeded to study their rhodium complexes. *Ortho*-substituted *o*(CF_3)P ligand reacted with $Rh_2(CO)_4Cl_2$ through the bridge splitting route to yield monometallic tetra-co-ordinated rhodium chlorocarbonyl complex having two phosphorus ligands in mutual *trans* position bonded in monodentate fashion, [Rh(CO)Cl(oCF_3P)$_2$] (**1**) (Fig. 3). Selected interatomic bond distances and

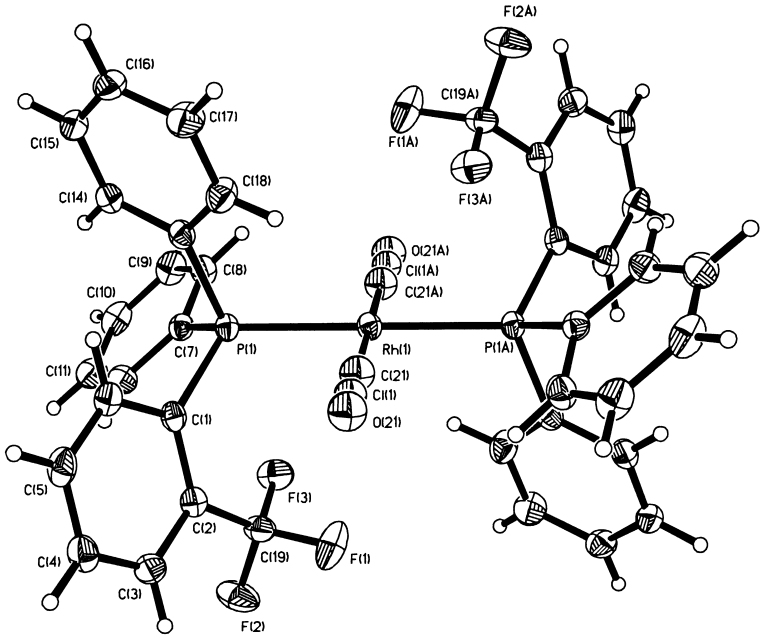

Fig. 3. Ortep drawing of compound **1** with thermal ellipsoids at 50% level.

angles are given in Table 3. The structure shows a planar geometry around the rhodium atom with a slight deviation from ideal. As is characteristic of $Rh(CO)Cl(PX_3)_2$ species, the compound shows disorder along the carbonyl/chloro axis. It gives a strong CO stretching vibration (IR) at 1977 cm^{-1}, and the ^{31}P NMR spectrum shows a doublet at 37.5 ppm with Rh–P coupling constant of 136 Hz.

The triply *para*-substituted $p(CF_3)_3P$ ligand afforded dinuclear chloro-bridged complex $[Rh(CO)_2Cl(p(CF_3)_3P)_2]_2$ (**2**). The carbonyl stretching frequency (IR) was shifted to higher field 1999 cm^{-1} relative to **1** due to the more electron-withdrawing ligand. Similarly, the ^{31}P NMR-shift was found at higher field (46.9 ppm) with higher $^1J_{Rh-P}$ of 170 Hz.

4. Discussion

4.1. Activity

The ligands induced different effects on the hydroformylation activity of 1-hexene and propene. Only the CF_3-modified ligands behaved alike with the two alkenes. Apparently, the changes in the stereoelectronic properties of the CF_3-modified ligands, and so also the properties of the respective rhodium complexes were significant enough to outstrip the individual properties of the two alkenes.

Even though the main purpose of the CF_3 substituents was to modify the electronic state of the phosphorus atom, the substitution also affected the cone angles of the *ortho*-substituted oCF_3P and $o(CF_3)_3P$ ligands. With both alkenes the oCF_3P modified catalyst system showed no activity most likely due to steric reasons. Co-ordination of the oCF_3P ligand (Fig. 3) shows that CF_3 groups are nearby the rhodium centre preventing the approach of alkenes. Similarly, sterically more-crowded $o(CF_3)_3P$ blocked the hydroformylation of propene.

However, the steric factors do not explain the behaviour of the corresponding *para*-substituted CF_3-modified ligands. Both the pCF_3P and the $p(CF_3)_3P$ ligand have a cone angle of 149° (the same as PPh_3) but pCF_3P gave zero conversion while $p(CF_3)_3P$ worked well with both substrates. The reason for this kind of behaviour is not clear. Possibly, the polarity of $p(CF_3)_3P$ resembles that of with PPh_3, leading to similar catalytic behaviour. In the case of pCF_3P, the lack of rhodium hydride formation could explain the inactivity.

The vast majority of published literature reports describe the isomerisation of 1-hexene to 2-hexenes [24,25] and even to 3-hexenes [9] concurrently with hydroformylation, whereafter hydroformylation of the isomers occurs (Fig. 1). With all tested ligands, the isomerisation activity was in line with the hydroformylation activity of the catalyst. Those catalysts (oOP and oOP(naf)$_2$ modified) that did not produce an equilibrium between 2- and 3-hexenes were also in general less reactive, yielding lower selectivity to aldehydes.

Strong σ-donor ligands oSP and oSP(naf)$_2$ yielded slightly higher hydroformylation activity with 1-hexene than did the less basic oOP and oOP(naf)$_2$ ligands. This is in contrast to the general belief that strongly basic phosphines are less active in hydroformylation [26,27]. It was shown in our previous paper [8] that both oSP and oNP bind bidentately to the rhodium, whereas oOP ligand co-ordinated monodentately (Fig. 4). Planar substructures formed as a result of bidentate co-ordination make the rhodium centre more accessible and may explain the enhanced hydroformylation activity. However, the oNP chelate complex with rhodium is considered to be weaker than that of oSP. Since nitrogen lacks π-orbitals and thus does not exhibit π-acceptor capability, the co-ordination might be more labile. This kind of hemilabile character, earlier proposed by Horner and Simons [28], allows oNP ligand to act — at least partly — monodentately during the catalytic cycle.

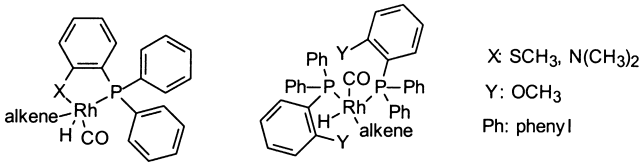

Fig. 4. Illustration of bidentate vs. monodentate binding.

Indeed, the chemoselectivity to aldehydes decreases in the order *o*SP, *o*NP and *o*OP, as does the bidentate character.

In propene hydroformylation with catalysts containing ligand with heterodonor group in *ortho* position, only the *o*NP modified catalyst led to reaction resembling that of the PPh_3 modified catalyst. We believe, for the reasons already stated above for 1-hexene, that the *o*NP ligand could possess hemilabile character and act as a monodentate ligand during the catalytic cycle.

We have previously shown [7] that in the hydroformylation of MMA with the *o*SP modified catalyst, the chelation control plays an essential role in determining the activity and regioselectivity of the reaction. Evidently, the chelation control is at work here: when the thiomethyl group is moved from *ortho* position (*o*SP) to the *para* position (*p*SP) or when the ligand contains bulky groups (*o*SP(naf)$_2$) that weaken the chelation, the catalytic activity is restored. Indeed, the plain steric stress of the *o*SP, *p*SP and *o*SP(naf)$_2$ ligands (the cone angles 158, 152 and 166°, respectively) is too similar to alone explain differences in the reactivity. At high ligand to rhodium ratios (L:Rh at least 5) the DPPB ligand acts as a monodentate ligand, whereas the DPPE ligand acts as a bidentate one [29]. This further reinforces our conclusion that under tested conditions, this type of small chelating bidentate ligands hindered hydroformylation of propene.

4.2. Regioselectivity

The effect of the modifying ligand on the regioselectivity of the reaction was individual for 1-hexene and propene. No analogy between the two substrates was found. In 1-hexene hydroformylation, the isomerisation had a dominant effect on the regioselectivity, whereas in propene hydroformylation the *n*:*i* ratio seemed mostly to depend on the direct stereoelectronic effect of the ligand in the hydroformylation transition state.

In propene hydroformylation, DPPB and *o*SP(naf)$_2$ modified the regioselectivity of the reaction relative to PPh_3. DPPB and *o*SP(naf)$_2$ favoured the formation of *n*-butanal most likely for steric reasons. Sterically, the PPh_2(anthr) ligand is more demanding than PPh_3, and the ^{31}P-shift differs markedly from that of PPh_3; however, comparison with the properties and catalytic behaviour of the other ligands, suggests that neither of these properties can really explain the obtained regioselectivity.

The binding mode discussed in the previous section (Fig. 4) also explains the differences in regioselectivity between *o*SP, *o*OP (*n*:*i* = 1.4 and 1.7) and *o*SP(naf)$_2$, *o*OP(naf)$_2$ (*n*:*i* = 1.4 and 2.0) in 1-hexene hydroformylation. According to complex studies, *o*SP and *o*SP(naf)$_2$ are bound bidentately yielding a planar substructure and a smaller and more accessible complex also capable of hydroformylating 2- and 3-hexenes, whereas *o*OP and *o*OP(naf)$_2$ are bounded monodentately resulting in a more hindered complex mainly hydroformylating 1-hexene [8].

The steric stress of the ligand does not totally explain the regioselectivity of the reaction in 1-hexene hydroformylation. Replacement of the phenyl rings with bulkier rings (PPh_2(anthr) and PPh(anthr)$_2$) caused the *n*:*i* ratio to increase slightly, but introduction of heterodonor groups to *ortho* position of the phenyl ring caused greater increase.

5. Conclusions

The effect of in situ introduced ligands was found to vary with reacting alkene. However, analogy between 1-hexene and propene was found with CF_3 modified ligands. In 1-hexene hydroformylation, isomerisation was the main reaction and the differences in the activity as well as the chemo- and regioselectivity were minor, whereas in propene hydroformylation even a small change in the ligand structure affected markedly the activity and regioselectivity of the catalyst system. In the case of propene, 1,4-bis(diphenylphosphino)butane and (*o*-thiomethylphenyl)bis(1-naphthyl)phosphine favoured the formation of *n*-butanal.

Acknowledgements

We gratefully acknowledge the financial support from Neste Chemicals. We wish to thank Ms. Päivi Joensuu and Ms. Sari Ek for the mass spectra and Ms. Johanna Suutari for performing part of the propene hydroformylation tests. The assistance of Ms. Liisa Saharinen in 1-hexene hydroformylation and preparation of rhodium complexes was most helpful.

References

[1] M. Diéguez, M.M. Pereira, A.M. Masdeu-Bultó, C. Claver, J.C. Bayón, J. Mol. Catal. A: Chem. 143 (1999) 111.
[2] C.P. Casey, G.T. Whiteker, M.G. Melville, L.M. Petrovich, J.A. Gavney Jr., D.R. Powell, J. Am. Chem. Soc. 114 (1992) 5535.
[3] L.A. Van der Veen, M.D.K. Boele, F.R. Bergman, P.C.J. Kamer, P.W.N. Van Leeuwen, K. Goubitz, J. Fraanje, H. Schenk, C. Bo, J. Am. Chem. Soc. 120 (1998) 11616.
[4] T. Fuchikami, I. Ojiama, J. Am. Chem. Soc. 104 (1982) 3527.
[5] W.R. Jackson, P. Perlmutter, G.-H. Suh, J. Chem. Soc., Chem. Commun. (1987) 724.
[6] M.M. Doyle, W.R. Jackson, P. Perlmutter, Aust. J. Chem. 42 (1989) 1907.
[7] H.K. Reinius, R.H. Laitinen, A.O.I. Krause, J.T. Pursiainen, Stud. Surf. Sci. Catal. 130 (2000) 551.
[8] P. Suomalainen, S. Jääskeläinen, M. Haukka, R.H. Laitinen, J. Pursiainen, T.A. Pakkanen, Eur. J. Inorg. Chem., (2000) 2607.
[9] C. Bianchini, P. Frediani, A. Meli, M. Peruzzini, F. Vizza, Chem. Ber./Recueil 130 (1997) 1633.
[10] A.M. Trzeciak, J.J. Ziolkowski, J. Mol. Catal. 34 (1986) 213.
[11] C.A. Tolman, Chem. Rev. 77 (1977) 313.
[12] G.R. Miller, A.W. Yankowsky, S.O. Grim, J. Chem. Phys. 51 (1969) 3185.
[13] K.C. Eapen, C. Tamborski, J. Fluorine Chem. 15 (1980) 239.
[14] M.J. Frisch, G.W. Trucks, H.B. Schlegel, P.M.W. Gill, B.G. Johnson, M.A. Robb, J.R. Cheeseman, T. Keith, G.A. Petersson, J.A. Montgomery, K. Raghavachari, M.A. Al-Lahman, V.G. Zakrzewski, J.V. Ortiz, J.B. Foresman, J. Cioslowski, B.B. Stefanov, A. Nanayakkara, M. Challacombe, C.Y. Peng, P.Y. Ayala, W. Chen, M.W. Wong, J.L. Andres, E.S. Replogle, R. Gomperts, R.L. Martin, D.J. Fox, J.S. Binkley, D.J. Defrees, J. Baker, J.P. Stewart, M. Head-Gordon, C. Gonzales, J.A. Pople, Gaussian, Inc., Pittsburgh, PA, USA, 1995.
[15] Sybyl 6.03; Tripos Associates, 1699 S. Hanley Road, Suite 303, St. Louis, MO 63144, USA.
[16] J.A. Cleverty, G. Wilkinson, Inorganic Syntheses, Vol. 8, McGraw-Hill, New York, 1966, p. 211.
[17] Z. Otwinowski, W. Minor, Processing of X-ray Diffraction Data Collected in Oscillation Mode, Methods in Enzymology, Vol. 276, in: C.W. Carter Jr., R.M. Sweet (Eds.), Macromolecular Crystallography, Part A, Academic Press, New York, 1997, pp. 307–326.
[18] A. Altomare, M.C. Burla, M. Camalli, G.L. Cascarano, C. Giacovazzo, A. Guagliardi, A.G.G. Moliterni, G. Polidori, R. Spagna, J. Appl. Cryst. 32 (1999) 115.
[19] L.J. Farrugia, WinGX, Version 1.61 — A Windows Program for Crystal Structure Analysis, University of Glasgow, Glasgow, UK, 1998.
[20] G.M. Sheldrick, SHELXL97, Program for Crystal Structure Refinement, University of Göttingen, Germany, 1997.
[21] G.M. Sheldrick, SHELXTL, Version 5.1, Bruker Analytical X-ray Systems, Bruker AXS, Inc., Madison, WI, USA, 1998.
[22] C.L. Yaws, X. Pan, Chem. Eng. (1992) 130.
[23] C.L. Yaws, Thermodynamic and Physical Property Data, Gulf Publishing Company, Houston, 1992, 217 pp.
[24] M.E. Davis, P.M. Butler, J.A. Rossin, J. Mol. Catal. 31 (1985) 385.
[25] R. Lazzaroni, P. Pertici, S. Bertozzi, G. Fabrizi, J. Mol. Catal. 58 (1990) 75.
[26] J.D. Unruh, J.R. Christenson, J. Mol. Catal. 14 (1982) 19.
[27] W.R. Moser, C.J. Papile, D.A. Brannon, R.A. Duwell, S.J. Weininger, J. Mol. Catal. 41 (1987) 271.
[28] L. Horner, G. Simons, Z. Naturforsch. 39b (1984) 497.
[29] D.E. Hendriksen, A.A. Oswald, G.B. Ansell, S. Leta, R.V. Kastrup, Organometallics 8 (1989) 1153.
[30] D.W. Meck, G. Dyer, M.O. Workman, Inorg. Synth. 16 (1976) 168.
[31] E. Meintjies, E. Singleton, R. Schmutzler, S. Afr. J. Chem. 38 (1985) 115.
[32] G. Dryer, D.W. Meek, J. Am. Chem. Soc. 89 (1967) 3983.
[33] R.H. Laitinen, V. Heikkinen, M. Haukka, A.M.P. Koskinen, J. Pursiainen, J. Organomet. Chem. 598 (2) (2000) 235.
[34] J. Wesemann, P.G. Jones, D. Schomburg, L. Heuer, R. Schmutzler, Chem. Ber. 125 (1992) 2187.